

## Thulium (III) Hexacyanoferrate Star Fruit-Like Structure Modified Electrode for L-Cysteine Electrochemical Sensor

Mani Sakthivel, Mani Sivakumar, Shen-Ming Chen\*, Wei Lun-Cheng

Electroanalysis and Bioelectrochemistry Lab, Department of Chemical Engineering and Biotechnology, National Taipei University of Technology, Taipei 10608, Taiwan.

\*E-mail: [smchen78@ms15.hinet.net](mailto:smchen78@ms15.hinet.net)

Received: 26 May 2016 / Accepted: 5 July 2016 / Published: 7 August 2016

---

We report the preparation of star fruit-like thulium hexacyanoferrate (TmHCF) by using one-step electrochemical deposition in cyclic voltammetry technique. The electrochemically deposited star fruit-like TmHCF is exhibit unique electrocatalytic activity towards the detection of L-cysteine (L-Cys). The as-prepared TmHCF was characterized using different techniques such as scanning electron microscopy (SEM), X-ray diffraction (XRD), electrochemical impedance spectroscopy (EIS). The electrochemical activity of star fruit-like TmHCF was studied using cyclic voltammetry (CV), and differential pulse voltammetry (DPV). The modified electrode shows a considerable linear range, sensitivity and detection limit of about 0.5 to 8.92  $\mu\text{M}$ , 48.479  $\mu\text{A } \mu\text{M}^{-1} \text{cm}^{-2}$  and 16 nM respectively. Furthermore, the modified electrode was tested in the real samples analysis in urine and river water samples.

---

**Keywords:** Thulium hexacyanoferrate (TmHCF), electrochemical sensor, L-cysteine.

### 1. INTRODUCTION

L-cysteine (L-Cys) is the sulfur containing amino acid with formula  $\text{C}_3\text{H}_7\text{NO}_2\text{S}$  which plays an important role in living systems especially the biological activities of enzymes and proteins [1,2] and it act as an antioxidant which may prevent the liver diseases [3]. L-Cys found in many foods such as soybeans, beef, onions, sunflowers seeds, chicken, and oats. The referred amount of L-cys for daily intake of about 4.1mg. A person with 70kg weighting should consume around 287mg of L-Cys per day. It has found in many pharmaceutical applications; specifically, it is used in antibiotics, for the treatment of skin damage, and as a radioprotective agent. The shortage of the L-Cys causes much illness, such as slowed growth in children, de-pigmentation of hair, edema, lethargy, liver damage, and loss of muscle and sever skin problem [4, 5]. Hence, the probing of L-cys in body fluids, pharmaceuticals, and food samples is very significant [6]. Different techniques are using for the

determination of L-Cys such as flow injection method [7,8], capillary column liquid chromatography [9], pulse amperometric determination [10], electrochemiluminescence analysis [11] and electrochemical technique [12]. Among these all, the electrochemical techniques have considered as the promising technique owing to the relatively low cost, simplicity, low time consuming, high sensitivity, and selectivity [13].

Metal hexacyanoferrate is the type of stable coordination compounds with fcc lattice. Owing to the good stability, favorable capacitive behavior, photo reversible enhancement of magnetization, unique degradation efficiency, good selectivity and sensitivity, the metal hexacyanoferrate focused on different applications such as supercapacitor [14], battery [15], Electrocatalysis [16], photomagnetic and magneto optic devices [17], photocatalytic devices [18] and sensor [19]. In order to extend the application of metal hexacyanoferrate in the field of biosensor, the new types of rare metal hexacyanoferrate are developing with high stability of metal cyanide, cation exchange properties, efficient ionic conductivity and reversible redox properties [20, 21]. In 1994, karyakin *et al.*, reported the first research article based on the application of metal hexacyanoferrate for glucose biosensor with high sensitivity and selectivity. In the past decades, many types of metal hexacyanoferrate have been prepared using different preparation methods such as reverse micelles [22,23], simple chemical co precipitation technique [24], biocatalyst reaction [25], and electrochemical deposition. Among these all preparation methods, electrochemical deposition is simple cost and low time consuming technique to prepare the metal hexacyanoferrate with different morphology such as microstar like dysprosium hexacyanoferrate [26], flower like samarium hexacyanoferrate [27], flower and christmas tree like cerium hexacyanoferrate [28], yttrium (III) hexacyanoferrate micro flowers [29], switching structures of praseodymium hexacyanoferrate [30].

In this work, we reported a star fruit like thulium hexacyanoferrate (TmHCF) modified electrode by an electrochemical deposition technique using different electrolytes contain ferricyanide solution with  $\text{Tm}^{3+}$ . The electrochemically deposited micro flower TmHCF exhibits considerable sensitivity towards the sensing of L-cysteine. In addition, only a few reports are available for the synthesis, characterization and application of TmHCF for electrochemical sensor. Zuchao Meng *et al.*, reported TmHCF based glucose electrochemical sensor. However, the further studies are carried out to prepare the TmHCF with different morphology with improved electrocatalytic activity.

## 2. EXPERIMENTAL SECTION

### 2.1. Materials

L-cysteine and Thulium (III) chloride hexahydrate were purchased from Sigma Aldrich.  $\text{K}_3\text{Fe}(\text{CN})_6$  was purchased from Wako pure chemical industries. Electrocatalytic studies were carried out in 0.5 M KCl solution. All the solutions were prepared using doubly distilled water. All chemicals are analytical grade and used as received without any further purification.

## 2.2. Apparatus

Scanning Electron Microscopy (SEM) was performed using Hitachi S-3000 H electron microscope. Energy dispersive X-ray (EDX) spectrum was recorded using HORIBA EMAX X-ACT that was attached with Hitachi S-3000 H scanning electron microscope. XRD characterization was carried out using XPERT-3 diffractometer with Cu K $\alpha$  radiation ( $\lambda = 1.54 \text{ \AA}$ ). The Cyclic Voltammetry (CV) studies were performed by using CHI1205B electrochemical analyzer and Differential Pulse Voltammetry study were performed by using CHI900 electrochemical analyzer. Conventional three-electrode system was used for the electrochemical experiments, glassy carbon electrode (GCE) was used as a working electrode, a saturated Ag/AgCl electrode used as a reference electrode and a platinum electrode used as the auxiliary electrode. All measurements were carried out at room temperature.

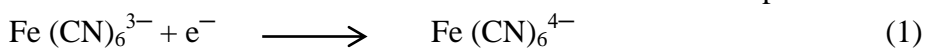
## 2.3. Preparation of TmHCF modified glassy carbon electrode (GCE)

The TmHCF modified GCE was prepared by an electrodeposition method using a CV technique. To prepare the star fruit-like TmHCF modified GC electrode, first GCE was polished with alumina on polishing cloth followed by washing in DD water and ethanol. The polished GCE was placed in 5mM TmCl<sub>3</sub>.H<sub>2</sub>O and K<sub>3</sub>Fe(CN)<sub>6</sub> in containing 0.1M KCl electrolyte. 20 consecutive cyclic voltammogram scans were performed between a potential range of 0.8 and -0.2 V at a scan rate of 50 mVs<sup>-1</sup>. The star fruit-like TmHCF were electrochemically deposited on the GCE surface. Then, the TmHCF modified GCE was rinsed with water and dried at room temperature. Thus, the fabricated GCE was used for further electrochemical studies.

## 3. RESULTS AND DISCUSSION

### 3.1. Electrochemical deposition of TmHCF

TmHCF was synthesized by using a simple method of cyclic voltammograms electrochemical deposition is shown in Fig. 1. The uniform deposition of TmHCF on the GCE surface confirmed due to the presents of redox peak. The peaks at +0.2 and 0.33 V implies the reduction of Fe (CN)<sub>6</sub><sup>3/4-</sup> and the corresponding peaks at +0.28 and 0.5 V with decreasing currents in the redox couple implies the oxidation reaction of the Fe(CN)<sub>6</sub><sup>3/4-</sup> in the solution. The Tm<sup>3+</sup> ions presents in the solution eagerly react with Fe (CN)<sub>6</sub><sup>4-</sup> ions and deposited on the electrode surface, the second redox couple indicates the reduction process of Tm[Fe (CN)<sub>6</sub>] is the contribution to the deposition of K[TmFe(CN)<sub>6</sub>] on the electrode surface. The formation of TmHCF mechanism can be expressed as follows; [26-30]



To investigate the deposition process, using the equal amount of (5 mM) thulium and hexacyanoferrate containing 0.1 M KCl solution at the cycle deposition between 0.8 to -0.2 V at a scan

rate of  $50 \text{ mV s}^{-1}$ . On other hand, for the different amount no redox peak observed, but if the potential change, the redox peak may be appear faintly (figures not shown). The optimal amount of MHCF deposition was found only for 5 mM metal precursor which enhances the reversible process during the deposition and the same concept was used in this study.

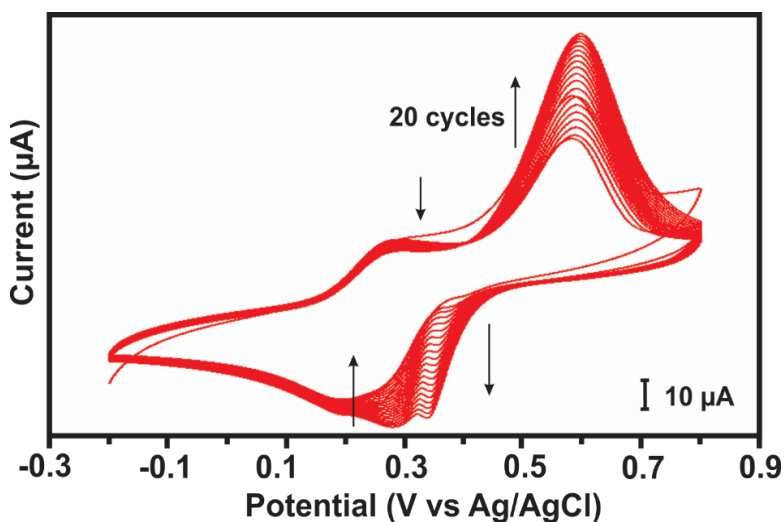


**Figure 1.** Electrodeposited TmHCF modified electrode in 0.1 M KCl solution containing 5 mM  $\text{TmCl}_3 \cdot 6\text{H}_2\text{O}$  and  $\text{K}_3 \text{Fe}(\text{CN})_6$  solution. CV curves were recorded for 20 cycles consecutives between 0.8 to -0.2 V at scan rate of  $50 \text{ mVs}^{-1}$ .

### 3.2. Surface morphology of TmHCF

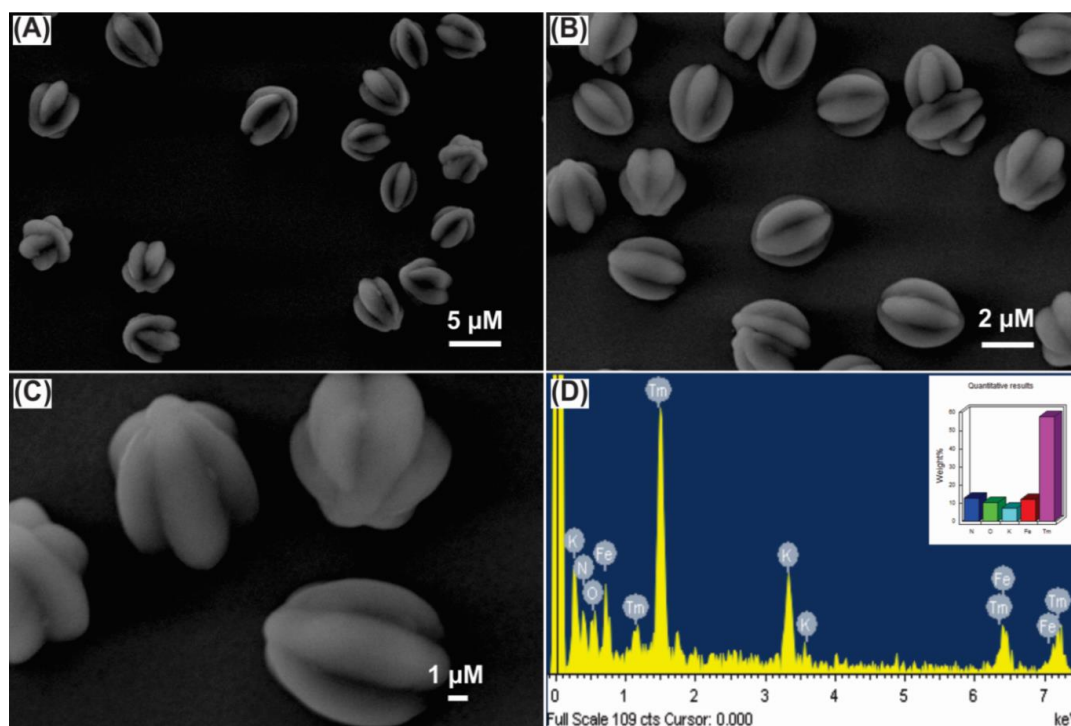


**Figure 2.** Surface morphology of TmHCF using SEM at different magnification images (A-C), SEM affiliated EDX spectrum (D).

Surface morphology of TmHCF was analyzed by SEM and SEM affiliated EDX spectra. The star fruit like TmHCF was deposited at cyclic voltammograms using 20 consecutive cycles and the different number of cycles were carried out during the deposition to confirm the growth of  $\text{TmFe}(\text{CN})_6$  on the surface of GCE. The TmHCF were observed with star fruit-like structure, which shown in Fig. 2. Moreover, the SEM affiliated EDX spectrum confirmed the presence of  $\text{TmFe}(\text{CN})_6$  and give the weight percentage of constituents in  $\text{TmFe}(\text{CN})_6$ . Here the Tm weight % of 57.71, Fe weight % of 12.08, potassium weight % of 7.20. These results were recorded on  $\text{TmFe}(\text{CN})_6$  deposited ITO surface.

### 3.3. Different electrolyte deposition for TmHCF

To investigate the morphological changes according to the nature of the electrolyte, the GCE placed in different types of electrolytes such as 0.1 M KCl, HCl, LiCl and NaCl during the deposition process. The different morphologies of TmHCF were observed for corresponding electrolytes and shown Fig. 3 (A-D). From the SEM images KTmHCF were observed clearly as star fruit-like structure as shown in Fig. 3 (A). The unequal size of cubic and spherical like structures were observed for HTmHCF and the fewer amounts of particles were deposited on the modified electrode surface as shown Fig. 3 (B). Moreover, the unequal size of particles and star like structures for LiTmHCF as shown Fig. 3 (C) and the star-like structure for NaTmHCF shown in Fig. 3 (D). Here, the LiTmHCF and NaTmHCF are deposited on the GCE surface with fewer amounts of particles only. Further, the  $\text{H}^+$ ,  $\text{Na}^+$ , and  $\text{Li}^+$  electrolyte was observed in the particle size, shape, stability and electrochemical properties for few parts only. The uniform morphology changes observed in the order of  $\text{K}^+ > \text{Na}^+ > \text{Li}^+ > \text{H}^+$ . Hence, in this work  $\text{K}^+$  electrolyte was used to obtain the well uniform morphology and for all further experiment.

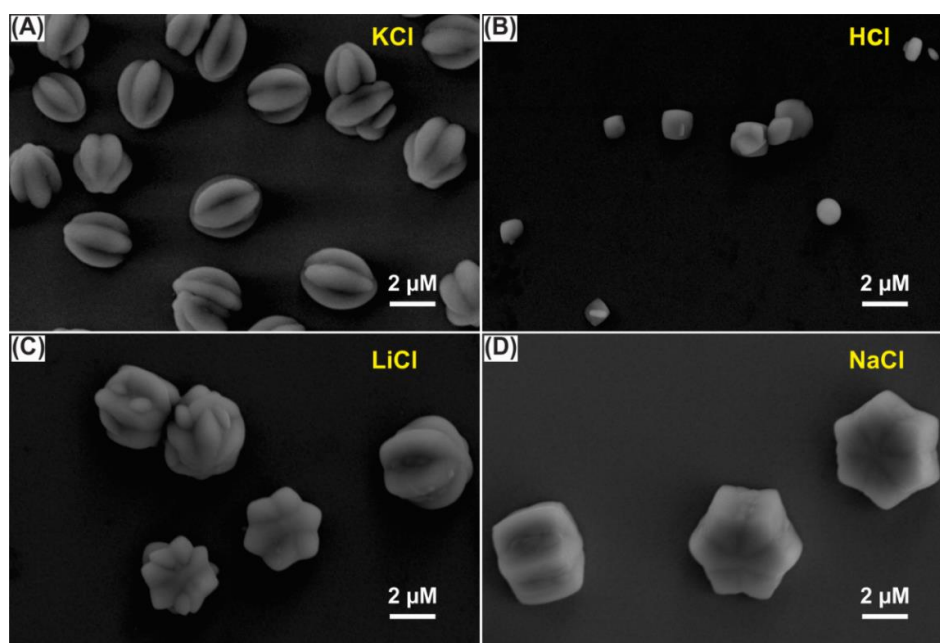


**Figure 3.** The effect of different electrolyte such as 0.1 M (KCl, HCl, LiCl and NaCl) studies was used by SEM images (A-D).

3.4. XRD and EIS Characterization of star fruit like TmHCF

In the X-ray diffraction pattern the Fig. 4 (A) shows the major peaks with corresponding crystal planes (211), (222), (400), (440) and (640) for the TmHCF film. The result indicates that  $Tm^{3+}$  ions are successfully deposited on the ITO plate. The electrochemical impedance spectroscopies (EIS) carried out to determine the electron transfer behavior of TmHCF modified electrode. From the Nyquist plot and Randles circuit the real component ( $Z_{re}$ ) and imaginary component ( $Z_{im}$ ), charge transfer resistance ( $R_{ct}$ ), solution resistance ( $R_s$ ) and capacity ( $C_{dl}$ ) were obtained for TmHCF modified GC electrode. The  $R_{ct}$  value obtained for bare GCE of about 138.6  $\Omega$ . Then, the  $R_{ct}$  value for TmHCF modified GC electrodes of about 713.68, 661.71, 363.84, 316.54  $\Omega$  by varying the number deposition cycles 5, 10, 15, and 20 respectively is shown in Fig. 4 (B). Finally, the low charge transfer resistance  $R_{ct}$  obtained for 20 cycles.

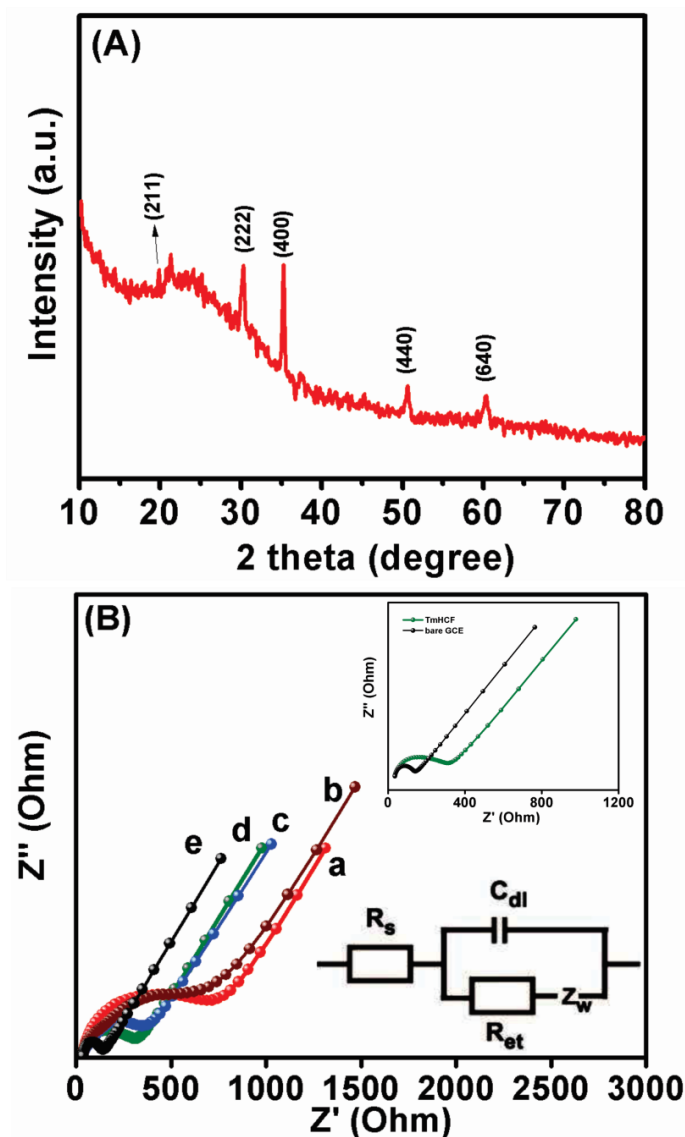


**Figure 4.** (A) XRD pattern, (B) EIS Spectrum analysis of different modified electrode by using 0.5 M KCl solution in containing 5 mM  $[Fe(CN)_6]^{3/4-}$  electrolyte.

## 3.5. Electrochemical studies of TmHCF-GCE

Fig. 5 (A, C) shown the CV curve for TmHCF-GCE for both with and without of L-Cysteine (145  $\mu\text{M}$ ) in a 0.5 M KCl solution at a different scan rate of 50-500  $\text{mVs}^{-1}$ . The inset in fig. 5 (A, C) shown the linear calibration plot for the square root of scan rate vs current. The linear regression equation were calculated to anodic and cathodic value of with presents  $R^2 = 0.9869, 0.9677$  and without presents of  $R^2 = 0.9914, 0.9989$ . Here, the increasing current values were observed with increases scan rates and also the peaks potentials were shifted to positive side. The result implies the kinetic of overall process were controlled by diffusion process.

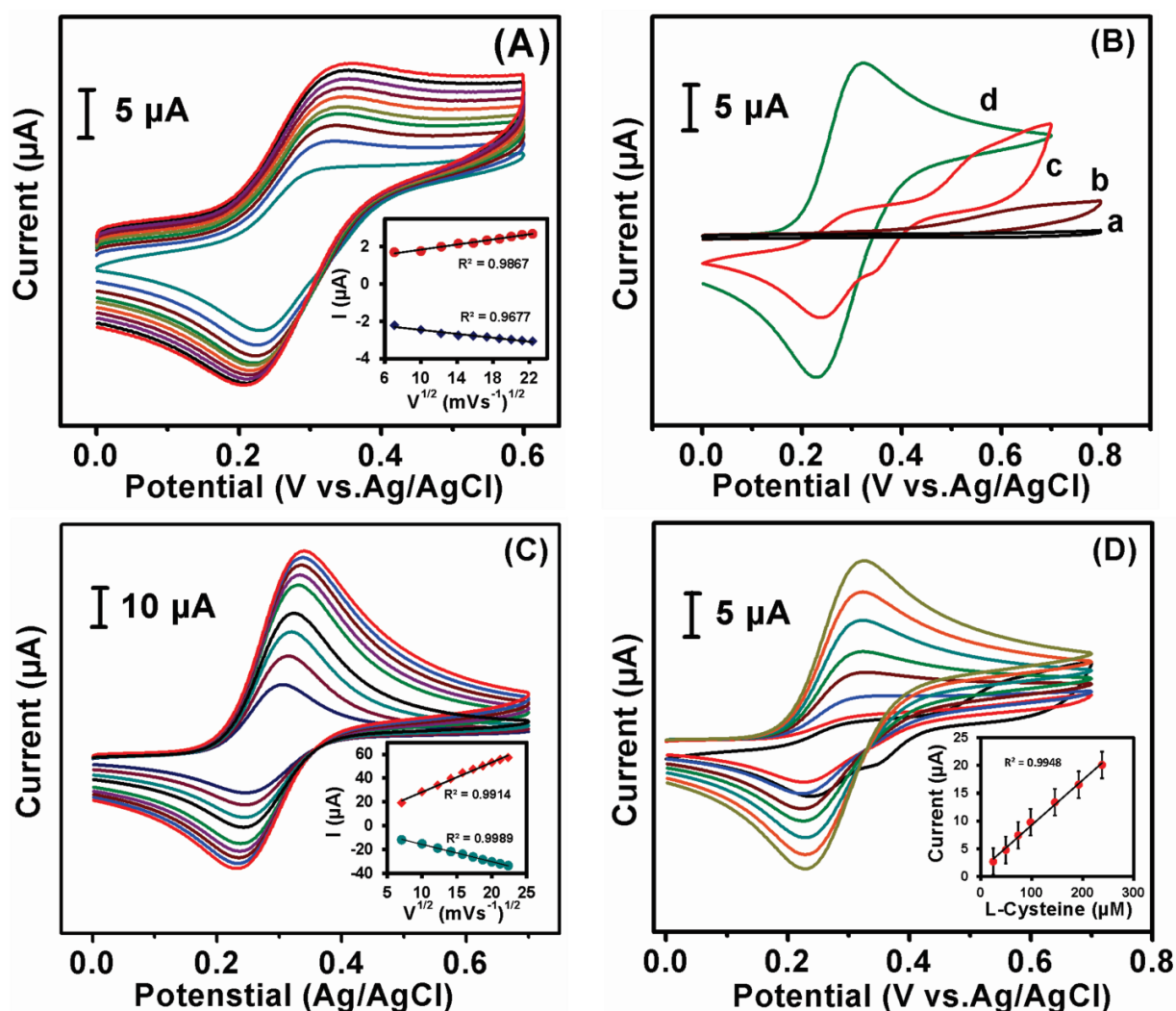


**Figure 5.** CV curves of different scan rate from 50-500  $\text{mVs}^{-1}$  at the without and with presents of (145  $\mu\text{M}$ ) L-cysteine (A, C) (inset: the corresponding calibration plots were calculated by the square root of scan rate vs current). CV curves of film comparison for (a) bare GCE only, (c) blank of TmHCF-GCE, (b) bare GCE, (d) TmHCF-GCE at the presents of (145  $\mu\text{M}$ ) L-cysteine, (B). CV Curves of different addition to L-Cysteine (inset: the corresponding calibration plot was calculated by different concentration of l-cysteine vs current). All experiments were during the 0.5 M KCl electrolyte at  $\text{N}_2$ -saturated.

CV curves for film comparison of the different electrode were studied by a 0.5 M KCl solution of L-Cysteine (145 $\mu$ L) at a scan rate of 50 mVs<sup>-1</sup>, as shown in fig. 5 (B). (a) bare GCE, (c) TmHCF-GCE with absence of L-cysteine, (b) bare GCE and (d) TmHCF-GCE with presents of L-Cysteine (145 $\mu$ L) in 0.5 M KCl solution at a scan rate of 50 mVs<sup>-1</sup>. Here, TmHCF-GCE shows the better redox response for L-cysteine than bare GCE. Fig 5 (D) shown the CV curves of TmHCF-GCE electrode for varying the concentration of L-cysteine with increasing redox current. The linear calibration plot was calculated for different concentration vs current. The linear calibration value were determined of about  $R^2 = 0.9948$ .

### 3.6. DPV studies of TmHCF-GCE

The TmHCF-GCE were studied by a DPV curves with increasing the concentration of L-cysteine in N<sub>2</sub> saturated 0.5 M KCl electrolyte at scan rate of 50 mVs<sup>-1</sup>, as shown Fig. 6. The inset shows the corresponding calibration plot for different concentration vs current. The linear calibration plot with the value of  $R^2 = 0.9837$  and the linear range were observed from 0.5 to 8.92  $\mu$ M. the Low detection limit and sensitivity were calculated to be 16 nM and 48.479  $\mu$ A  $\mu$ M<sup>-1</sup> cm<sup>-2</sup>, respectively. The obtained results were compared with previously reported literature and shown in table 1.

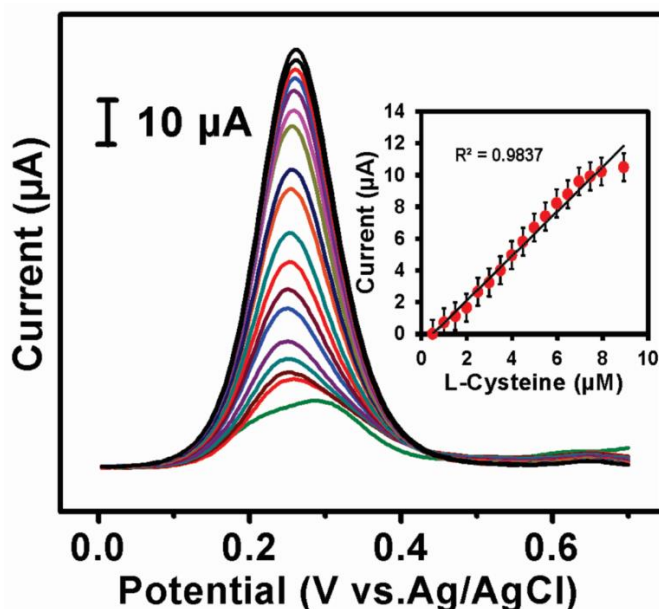


**Figure 6.** DPV curves of different concentration of L-cysteine for 0.5 M KCl electrolyte at N<sub>2</sub> saturated at the scan rate of 50 mVs<sup>-1</sup> (inset: the corresponding calibration plot was calculated by using different concentration vs current).

### 3.7. Repeatability, reproducibility and stability

The repeatability of the TmHCF-GCE modified electrode for L-Cysteine sensor was observed from CV measurements in the same electrolyte conditions. The as prepared modified electrodes exhibit

good repeatability with a relative standard deviation (RSD) of three following measurements. Here, the modified electrode was observed excellent reproducibility of the RSD value 4.4% for three individual electrode measurements. The modified electrodes show better stability in the same 0.5 M KCl electrolyte solution. The constant oxidation peak current obtained for the modified electrode towards sensing of L-Cysteine for the two consecutive days and the 91% of peak current remain same for one weeks (figure not shown), which is showing an exceptional storage stability TmHCF-GCE modified electrode.

**Table 1.** Comparison of different modified electrodes for the detection of L-Cysteine.

Modified electrodes	Techniques	LOD ( $\mu\text{M}$ )	Sensitivity ( $\mu\text{A } \mu\text{m}^{-1} \text{cm}^{-2}$ )	Linear range ( $\mu\text{M}$ )	Ref.
Cu-CoHCF	CV	4	-	6-1000	31
MWCNT-FeTsPc/GCE	Amperometry	1	0.176	10-200	32
Q-AgNPs-GNs-GCE	DPV	0.28	-	0.9-12	33
PPy/GQDs@PB/GF	Amperometry	0.15	0.4	50-1000	34
YHCF NP/MWNT/Nafion	Amperometry	0.16	0.1015	0.20-11.4	35
MoS <sub>2</sub> /PDDA-MC/GCE	Amperometry	0.090	-	0.45-155	36
[PEI/PSS] <sub>2</sub> /Au@2Ag/[PEI/P <sub>2</sub> Mo <sub>17</sub> V] <sub>2</sub> /ITO	Amperometry	0.027	1.7946	0.025-7.6	37
TmHCF/GCE	DPV	0.016	48.479	0.5-8.92	This work

### 3.8 Real sample analysis

**Table 2.** Real sample analysis with TmHCF-GCE.

Real samples	Analyte	Added ( $\mu\text{M}$ )	Found ( $\mu\text{M}$ )	Recovery (%)
Human urine	L-Cysteine	20	19.5	97.5
		40	49.1	98.2
		60	58.7	97.81
River water	L-Cysteine	50	49.01	98.02
		100	141.5	99.5
		300	291.06	97.02

The TmHCF-GCE was tested in the real sample analysis in urine and river water samples by using the standard addition method. The L-cysteine was contained in the urine sample within the ranges of 0.03-0.3 mmol/24h. The different addition of urine sample was added in TmHCF-GCE and the results shown in table 2. Furthermore, the same experiment was carried out in the river water

samples and its corresponding results also given (table 2). Hence, the modified electrode is well detected in the real sample.

#### 4. CONCLUSIONS

In this report, star fruit-like TmHCF was successfully synthesized in electrochemical deposition by using cyclic voltammetry technique. The star fruit like TmHCF-GCE found as the promising electrode for L-cysteine sensor. The nature of different electrolyte has played an important role to obtain the different morphology of TmHCF during the deposition which is confirmed by SEM. The crystallinity and the presents of constituents were determined using XRD and SEM affiliated EDX. Finally, the electrochemical activity such as sensitivity, low detection limit and linear range of TmHCF-GCE towards L-cysteine probed using CV and DPV technique.

#### ACKNOWLEDGMENTS

Financial supports of this work by the Ministry of Science and Technology, Taiwan (NSC101-2113-M-027-001-MY3 to SMC) is gratefully acknowledged.

#### Reference

1. N. Teshima, T. Nobuta and T. Sakai, *Anal. Chim. Acta.*, 438 (2001) 21.
2. Xu Chen, Yi Yang and Mingyu Ding, *Anal. Chim. Acta*, 557 (2006) 52.
3. S. Shahrokhian and S. Bozorgzadeh, *Electrochim. Acta*, 51 (2006) 4271.
4. B. Li, D. Wang, C. Xu, and Z. Zhang, *Microchim. Acta*, 149 (2005) 205.
5. F. A. S. Silva, M. G. A. Silva a, P. R. Lima, M. R. Meneghetti, L. T. Kubota and M. O. F. Goulart, *Biosens. Bioelectron.*, 50 (2013) 202.
6. N. Maleki, A. Safavi, F. Sedaghati and F. Tajabadi, *Anal. Biochem.*, 369 (2007) 149.
7. C. Zhao, J. Zhang, and J. Song, *Anal. Biochem.*, 297 (2001) 170.
8. T. Pe' rez-Ruiz, C. M. Lozano, V. Toma's and J. Marti'n, *Talanta*, 58 (2002) 987.
9. A. E. Katrusiak , P. G. Paterson , H. Kamencic , A. Shoker and A. W. Lyon, *J. Chromatogr. B*, 758 (2001) 207.
10. J. B. Raoof, R. Ojani, H. Beitollahi, and R. Hosseinzadeh, *Anal. Sci.*, September 2006, VOL. 22 1213.
11. H. Niu, R. Yuan, Y. Chai, L. Mao, Y. Yuan, Y. Zhuo, S. Yuan and X. Yang, *Biosens. Bioelectron.*, 26 (2011) 3175.
12. H. Hosseini, H. Ahmar, A. Dehghani, A. Bagheri, A. Tadjarodi and A. R. Fakhari, *Biosens. Bioelectron.*, 42 (2013) 426.
13. H. Razmi and H. Heidari, *Anal. Biochem.*, 388 (2009) 15.
14. A. Safavi, S. H. Kazemi and H. Kazemi, *Electrochimica Acta*, 56 (2011) 9191.
15. M. H. Wong, Z. Zhang, X. Yang, X. Chen and J. Y. Ying, *Chem. Commun.*, 51 (2015) 13674-13677.
16. N. A. Sitnikova, M. A. Komkova, I. V. Khomyakova, E. E. Karyakina, and A. A. Karyakin, *Anal. Chem.*, 86 (2014) 4131.
17. S. Ohkoshi and K. Hashimoto, *J. Photochem. Photobiol. C: Photochem. Rev.*, 2 (2001) 71-88.
18. V. Jassal, U. Shanker, B. S. Kaith and S. Shankar, *RSC Adv.*, 5 (2015) 26141.
19. D. Ivekovi, S. Milardovi and B.S. Grabari, *Biosens. Bioelectron.*, 20 (2004) 872.
20. J. Zhang, J. Li, F. Yang, B. Zhang and X. Yang, *Sens. Actuator B*, 143 (2009) 373.

21. B. Haghighi, H. Hamidi and L. Gorton, *Sens. Actuator B*, 147 (2010) 270.
22. M. Yamada, T. Sato, M. Miyake and Y. Kobayashi, *Journal of Colloid and Interface Science*, 315 (2007) 369.
23. S. bastien Vaucher, J. Fielden, M. Li, E. Dujardin, and S. Mann, *Nano Lett.*, 2 (2002) 225.
24. F. Qu, M. Yang, Y. Lu, G. Shen and R. Yu, *Analytical and Bioanalytical Chemistry*, 386 (2006) 228.
25. Z. Meng, J. Zheng, Q. Sheng and X. Zheng, *Analytica Chimica Acta*, 689 (2011) 47.
26. M. Rajkumar, B. Devadas and S. M. Chen, *Electrochimica Acta*, 105 (2013) 439.
27. B. Devadas, S. Cheemalapati, S. M. Chen and M. Rajkumar, *RSC Adv.*, 4 (2014) 45895.
28. B. Devadas, M. Sivakumar, S. M. Chen, M. Rajkumar, and C. C. Hu, *Electroanalysis*, DOI: 10.1002/elan.201500208.
29. B. Devadas, S. M. Chen, *J Solid State Electrochem.*, DOI 10.1007/s10008-014-2715-5.
30. B. Devadas, M. Sivakumar, S. M. Chen, S. Cheemalapati, *Electrochimica Acta*, 176 (2015) 350.
31. A. Abbaspour, and A. Ghaffarinejad, *Electrochimica Acta*, 53 (2008) 6643–6650.
32. R. Devasenathipathy, V. Mani, S. M. Chen, K. Kohilarani, and S. Ramara, *Int. J. Electrochem. Sci.*, 10 (2015) 682 – 690.
33. H. R. Zare, F. J. Dehaghani, Z. Shekari, and A. Benvidi, *Applied Surface Science*, 375 (2016) 169–178.
34. L. Wang, S. Tricard, P. Yue, J. Zhao, J. Fang, and W. Shen, *Biosensors and Bioelectronics*, 77 (2016) 1112–1118.
35. L. Qu, S. Yang, G. Li, R. Yang, J. Li, and L. Yu, *Electrochimica Acta* 56 (2011) 2934–2940.
36. Z. Zheng, Q. Feng, J. Li, C. Wang, *Sensors and Actuators B*, 221 (2015) 1162–1169.
37. L. Zhang, L. Ning, Z. Zhang, S. Li, H. Yan, H. Pang, and H. Ma, *Sensors and Actuators B*, 221 (2015) 28–36.

© 2016 The Authors. Published by ESG ([www.electrochemsci.org](http://www.electrochemsci.org)). This article is an open access article distributed under the terms and conditions of the Creative Commons Attribution license (<http://creativecommons.org/licenses/by/4.0/>).